Nuclear Instruments and Methods in Physics Research B 358 (2015) 1–5

Contents lists available at ScienceDirect

Nuclear Instruments and Methods in Physics Research B

journal homepage: www.elsevier.com/locate/nimb

Influence of the interface on the magnetic properties of NiZn ferrite thin films treated by proton irradiation

X.D. Jiang [a,b], D.W. Guo [b], C.H. Zhang [a,*], X.L. Fan [b], G.Z. Chai [b], D.S. Xue [b,*]

[a] Institute of Modern Physics, Chinese Academy of Sciences, Lanzhou 730000, China

[b] Key Laboratory for Magnetism and Magnetic Materials of the Ministry of Education, Lanzhou University, Lanzhou 730000, China

ARTICLE INFO

Article history:
Received 10 January 2015
Received in revised form 18 March 2015
Accepted 7 May 2015

Keywords:
NiZn ferrite
Proton irradiation
Magnetic properties
Interface
Stress

ABSTRACT

In order to systematically investigate the influence of the interface on the magnetic properties, polycrystalline NiZn ferrite thin films were irradiated with 60 keV proton in the dose range from 5×10^{12} to 5×10^{16} ions/cm^2. A non-destructive approach by proton irradiation was found to finely adjust the magnetic properties of polycrystalline NiZn ferrite thin films such as coercivity, perpendicular magnetic anisotropy as well as the effective *g* value. The coercivity is about 725 Oe for high proton dose ferrite, which is twice larger than the unirradiated one. The ferromagnetic resonance measurements indicated that perpendicular magnetic anisotropy and the effective *g* value increase with the irradiation dose. Our finding indicates that all modifications of these magnetic properties were associated with the change of interface due to the diffusion and the stress induced by proton irradiation. The change of the effective *g* value is a result of lattice expansion and the decrease of the magnetic dipole interaction between the columnar grains. This work provides a feasible way to tailor the magnetic properties of thin films by ion irradiation and promotes investigations for the stability of magnetic thin film devices in space or unclear radiation environments.

1. Introduction

Ion irradiation is an effectual tool to produce controllable defects, structural disorder, stress, and phase transformations so as to modify the properties of materials. In the case of magnetic thin films treated by the ion irradiation, property modification is mainly due to two aspects: irradiation on magnetic materials and implantation in the substrate. Great efforts have been made in the investigation on the effects of ion radiation on magnetic materials in recent years [1–8]. However, few studies have focused on the influence of the interface on the properties of single-layer magnetic materials.

NiZn ferrite with the spinel structure is a soft magnetic ferrite material exhibiting large resistivity and high magnetic permeability, especially suitable for many applications at high frequency [9–12], e.g. antenna rods, suppression of electromagnetic interference, broad band transformers, etc [13,14]. In addition, NiZn ferrite materials can be also wide applied in space. So the study of ion irradiation on the NiZn ferrite material is essential. Some efforts have been made on the effects of ion radiation on ferrite in recent years [2,3,15,16], including the saturation magnetization (M_s), distribution of the magnetic moments, magnetic anisotropy and magnetic domain structure [2,3]. These results are essentially attributed to structural modifications which are based on the variation of magnetic material itself such as the crystalline phase and cation inversion in the ferrite thin films. However, the influence of the interface on the magnetic properties of ferrite thin films by ion irradiation is rarely considered.

In this paper, experiments of NiZn ferrite thin films with thickness ~200 nm irradiated by 60 keV proton were designed to investigate the effects of ion irradiation. The energy of 60 keV was chosen to guarantee proton pass through the ferrite layer and implant into the substrate. Influences on coercivity (H_c), perpendicular magnetic anisotropy as well as the effective *g* value were systematically investigated. An effective way to flexibly control magnetic properties of NiZn ferrite was introduced by adjusting the interface via different irradiation doses.

2. Material and methods

We have taken the effort of preparing nanocrystalline ferrite thin films by radio frequency magnetron sputtering. $Ni_{0.45}Zn_{0.55}Fe_2O_4$ thin films were chosen as the mature samples [17]. Samples with thickness ~200 nm were deposited onto Si

* Corresponding authors.
E-mail addresses: c.h.zhang@impcas.ac.cn (C.H. Zhang), xueds@lzu.edu.cn (D.S. Xue).

http://dx.doi.org/10.1016/j.nimb.2015.05.010
0168-583X/

(1 1 1) substrates by radio frequency (RF) magnetron sputtering at room temperature with a base pressure lower than 5×10^{-5} Pa.

The samples were irradiated with 60 keV proton in the dose up to 5×10^{16} ions/cm^2 at room temperature in a chamber with a vacuum of 10^{-5} Pa in the ECR-320 kV High-voltage Platform (the Institute of Modern Physics (IMP), Lanzhou). According to SRIM simulations [18], the mean projective range of the proton was R_p = 350 nm (straggling: 83 nm), i.e., the protons were almost completely implanted in the Si substrates through the thin films. The structural characterization of the as-deposited and irradiated samples was performed by grazing incidence X-ray diffraction (GIXRD, X'Pert pro Panalytical with Cu K_α radiation). The X-ray patterns were recorded by the step scanning with a step of 0.02° and a counting time of 6 s per step. Field emission scanning electron microscope (SEM, Hitachi S-4800) was employed to observe the morphology of the thin films. In addition, cross-sectional transmission electron microscopy using a FEI Tecnai TMG2F30 microscope was carried out for typical samples to collect the information concerning crystallographic structure. The static magnetic properties were studied using a vibrating sample magnetometer (VSM, microsense EV7 system). M_s and H_c were evaluated from the VSM measurements. The effective anisotropy field and dynamic magnetic properties of the films were investigated by a cavity ferromagnetic resonance (JEOL, JESFA300, 8.994 GHz).

3. Results and discussion

Fig. 1(a) shows the GIXRD patterns of the $Ni_{0.45}Zn_{0.55}Fe_2O_4$ ferrite thin films after irradiated with protons at various doses. It shows that all the samples are well-crystallized with spinel structure and the mean grain size calculated by Scherrer's formula is about 18 nm, independent on the irradiation dose. The lattice parameter (Fig. 1(c)) of as-deposited thin film is 8.381 Å, which is very close to that of bulk $Ni_{0.4}Zn_{0.6}Fe_2O_4$ [19,20]. There is an increasing trend in the lattice parameter after irradiation, although it is not very obvious. This is mainly due to the stress effects induced by proton irradiation, because the energy deposition is mainly the electronic stopping powers (S_e) in the thin films. The large transferred energy induces an unusual density of defects, stress and heat in the samples. In other words, the changes in lattice parameter demonstrate that the stress in the thin films varied with irradiation doses. Then the production, accumulation and relaxation of the stress induced by proton irradiation can explain the changes in lattice constant very well [3].

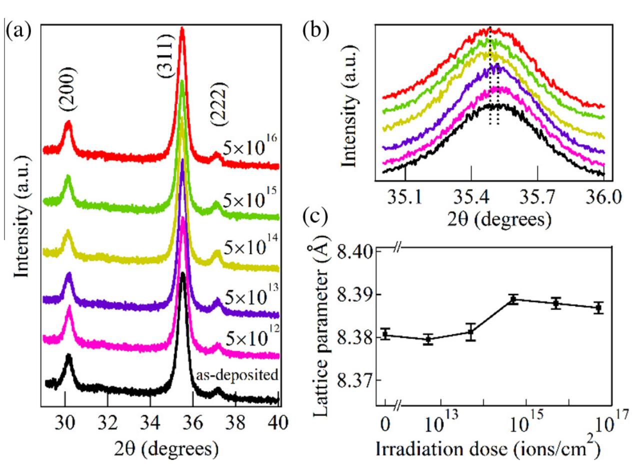

Fig. 1. (a) GIXRD patterns of NiZn ferrite thin films for the as-deposited sample and a series of different proton irradiation dose. (b) The (311) peak in detail. (c) The curves of the lattice parameter as a function of proton dose.

In order to investigate the irradiation effects on the morphology of the thin films, the surface and the cross-sectional morphology of the ferrite thin films are observed by the SEM. The surface images of the as-deposited and irradiated samples with a dose of 5×10^{16} ions/cm^2 are shown in Fig. 2(a and b). It is found that the mean crystalline sizes of the two samples are both about 20 nm and the surface morphology of the irradiated thin film was not obviously altered in comparison with the as-deposited samples. Fig. 2(c and d) show the cross-sectional SEM images of the as-deposited and irradiated samples with a dose of 5×10^{16} ions/cm^2, respectively. Both thin films have a relatively good packing density and a definite structure of columnar particles with their growing orientation perpendicular to the film plane. The thickness of as-deposited sample is about 200 nm and remains the same after irradiation. In conclusion, irradiation does not change the morphology of the thin films based on the SEM results.

The cross-sectional TEM images of the as-deposited and irradiated samples with a dose of 5×10^{16} ions/cm^2 are shown in Fig. 3. The images of Fig. 3(a and b) indicate that the thickness of the NiZn ferrite thin films remains unaffected after proton irradiation, and columnar grains grow perpendicularly to the substrates, which is consistent with the SEM results. It is also noted that there is a rough defect layer with thickness ~300 nm in the Si substrate after proton irradiation, which is consisted with the mean projected range of the proton calculated by SRIM. In fact, nuclear stopping powers (S_n) is dominant after ions passing through the thin films into the substrate. The elemental composition of the substrate can be altered in this process and many chemical and physical changes can be induced in the substrate by transferring the ion energy and momentum to the substrate materials. So the crystal structure of the substrate can be damaged or even destroyed by the energetic collision cascades. It is demonstrated that the defect layer induced by proton irradiation contains various defects and bubbles [21–24], which results in substrate expansion. Fig. 3(c and d) show the local enlarged high-resolution TEM images of the as-deposited and irradiated samples with a dose of 5×10^{16} ions/cm^2, respectively. It is revealed that the as-deposited sample is polycrystalline in the whole thickness range. The interface ~3 nm can be clearly observed in Fig. 3(c), and the diffusion between the film and Si (1 1 1) substrate is not obvious. Although the irradiated sample with a dose of 5×10^{16} ions/cm^2 still

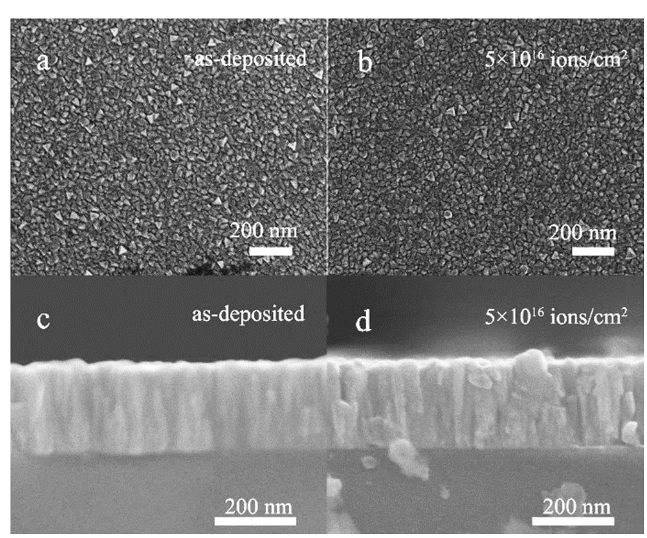

Fig. 2. (a) and (b) SEM images of the surface images of the as-deposited and irradiated samples with a dose of 5×10^{16} ions/cm^2 respectively. (c) and (d) The cross-sectional SEM images of the as-deposited and irradiated samples with a dose of 5×10^{16} ions/cm^2 respectively.

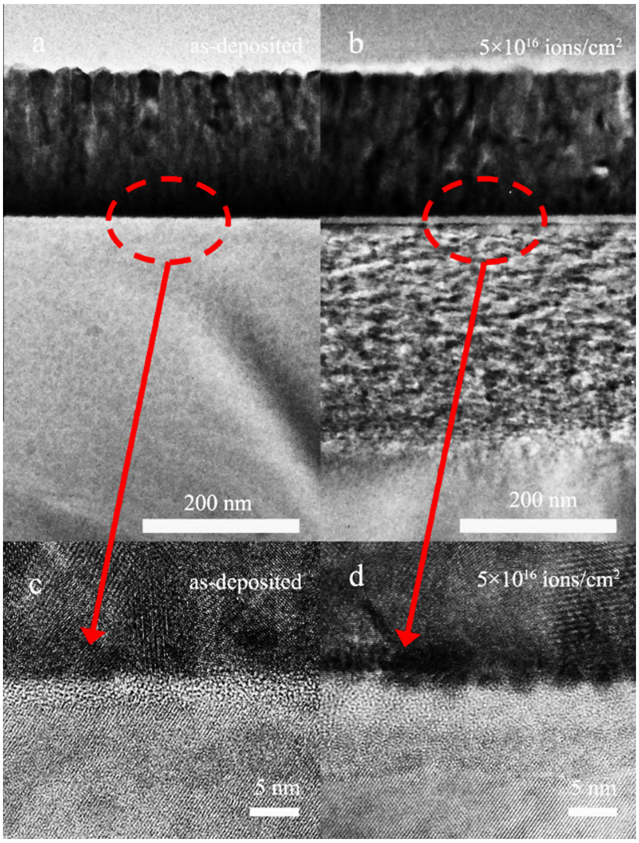

Fig. 3. (a) and (b) the cross-sectional TEM image of the as-deposited and irradiated samples with a dose of 5×10^{16} ions/cm^2 respectively. (c) and (d) High-resolution cross-sectional TEM image of the as-deposited and irradiated samples with a dose of 5×10^{16} ions/cm^2 respectively.

maintains a structure of columnar grains in the film, the ferrite diffuse into the interface along the direction of the columnar grains in Fig. 3(d). But irradiation-induced amorphous transformation is not discovered in the film due to the limited resolution of TEM. The interface of irradiated samples become unsmooth and indistinguishable due to the diffusion induced by irradiation. The thickness of this interface increases from 3 to 6 nm. The main reason is mutual diffusion between the film and the substrate and the transition of crystalline-to-amorphous [25–27] on the Si substrate surface induced by proton irradiation.

The in-plane magnetic hysteresis loops (M–H) are shown in Fig. 4(a). The coercivity (H_c) and the saturation magnetization

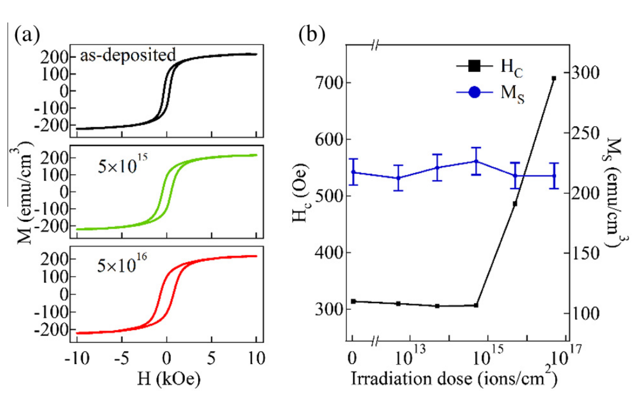

Fig. 4. (a) The in-plane magnetic hysteresis loops of the as-deposited and irradiated samples with a series of different proton dose. (b) M_s and H_c as a function of proton dose. The circle and square dots represent M_s and H_c, respectively.

(M_s), are revealed in Fig. 4(b). Taking into account the volume measurement error, the saturation magnetization (M_s) almost remains unchanged in all the irradiation conditions. The main reason is that the displacement energy of proton irradiation does not significantly change the occupancy distribution of the metallic cations in the thin films. The H_c does not change obviously when the dose is less than 5×10^{14}, but increases rapidly when the dose is higher. It has been known that the interface becomes unsmooth due to mutual diffusion according to TEM observations. Obviously the unsmooth interface is one reason contributed to the increasing coercivity with high doses of ion radiation because domain-wall pinning starts to affect the coercivity [28,29]. In addition, the rough defect layer (Fig. 3(b)) formed due to proton implantation in the Si substrate presents the tensile stress at the substrate [30], which can enhance the stress at the interface. This also contributes to the increase of the H_c. In our data, H_c has not change obviously when the dose is less than 5×10^{14} ions/cm^2 because the diffusion and the stress introduced by irradiation at low dose are not large enough. When the radiation dose reaches the particular threshold, the diffusion and the stress at the interface increase rapidly, and the H_c increases accordingly.

In order to investigate the variation of the anisotropy of the thin films, ferromagnetic resonance (FMR) measurement has been performed in a series of applied magnetic fields ranging from 0 to 9000 Oe. When the direction of applied magnetic field is rotated in film plane, the resonance field (H_{res}) does not changed. It is demonstrated that the samples are isotropic in film plane. However, H_{res} changes regularly when the direction of applied magnetic field is rotated out of the film plane. The direction of the applied field is initially in the direction of the thin film plane ($\theta_H = -90°$), then measurement was performed at an interval of 5° until the applied field direction returns back to the film plane ($\theta_H = 90°$). Fig. 5(a) is the transient inductive signal with the applied field in the normal direction of the thin film. The signal curves (Fig. 5(a)) are integrated and then fitted using a single Lorentzian function.

Fig. 5(b) shows that the out-of-plane angle (θ_H) dependence of the extracted the resonance field H_{res} and the inset depicts the field geometry. FMR was used to determine the value of the perpendicular magnetic anisotropy (PMA). The total free energy density can be expressed approximately in Eq. (1):

$$F = -HM_S[\cos\theta_M \cos\theta_H + \sin\theta_M \sin\theta_H \cos(\varphi_M - \varphi_H)] + 2\pi M_S^2 \cos^2\theta_M + K_\perp \sin^2\theta_M \quad (1)$$

Here the first term is Zeeman energy, the second term is the demagnetizing field energy, and the last term is the energy of perpendicular anisotropy. θ_H is the angle between the applied field and the normal direction of the thin film, θ_M is the angle between magnetization vector and the normal direction of the thin film, φ_M and φ_H are the azimuthal angles of M and H, $K_\perp$ is perpendicular anisotropy constant. Substituting the free energy density F into FMR frequency can be derived by Suhl and Smit in Eq. (2) [31,32]

$$\left(\frac{\omega}{\gamma}\right)^2 = \frac{1}{M_S^2 \sin^2\theta_M}\left[\frac{\partial^2 F}{\partial\theta_M^2}\frac{\partial^2 F}{\partial\varphi_M^2} - \left(\frac{\partial^2 F}{\partial\theta_M \partial\varphi_M}\right)^2\right] \quad (2)$$

Then we got the ferromagnetic resonance equation for out-of-plane measurement configuration ($\varphi_M = \varphi_H$). The resonance condition is expressed in Eq. (3)

$$\left(\frac{\omega}{\gamma}\right)^2 = H_{res}^{\parallel}\left(H_{res}^{\parallel} + 4\pi M_S - H_\perp\right)$$

$$\frac{\omega}{\gamma} = H_{res}^{\perp} - 4\pi M_S + H_\perp \quad (3)$$

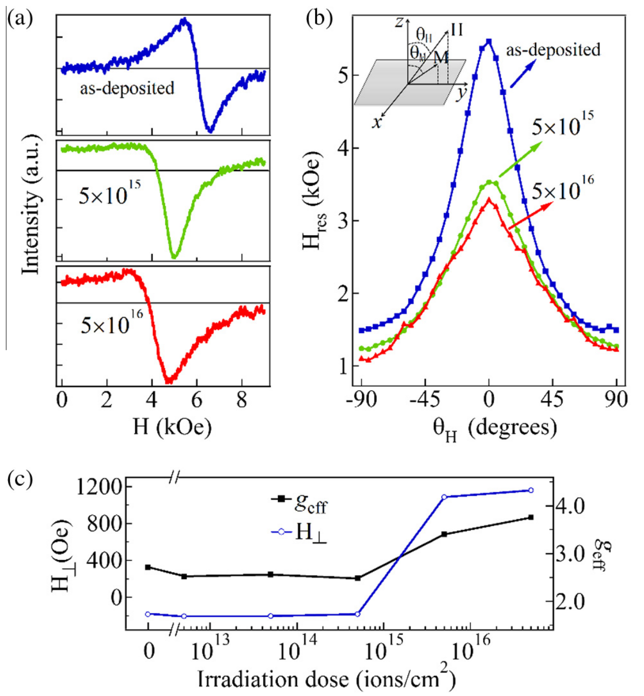

Fig. 5. (a) FMR spectra of the as-deposited and irradiated sample with a series of different proton dose when an applied field is normal to thin film. (b) H_{res} as a function of θ_H for the as-deposited and irradiated sample with a series of different proton dose. (c) $H_{\perp}$ and the g_{eff} of H_{res} as a function of proton irradiation dose for NiZn ferrite thin films.

$H_{res}^{\parallel}$ and $H_{res}^{\perp}$ are the resonance field when the applied field is parallel ($\theta_H = 90$ or -90) and perpendicular to the thin film plane ($\theta_H = 0$), respectively. The saturation magnetization $4\pi M_s$ are obtained by static VSM measurement. The PMA field $H_{\perp}$ and the gyromagnetic ratio γ can be acquired from Eq. (3), the effective g value (g_{eff}) is given by

$$g_{eff} = \frac{2m_e}{\mu_0|e|}\gamma \tag{4}$$

The $H_{\perp}$ and g_{eff} are extracted as a function of the proton dose in Fig. 5(c). The PMA field $H_{\perp}$ is negative and almost does not change when the irradiation dose is less than 5×10^{14} ions/cm^2, which implies that the magnetic anisotropy direction is in the thin film plane. When the radiation dose is higher than 5×10^{14} ions/cm^2, $H_{\perp}$ turns positive and increases dramatically, which indicates that the magnetic anisotropy shifts from in plane to out of plane. Since it is obvious that there is expansion of the substrate after proton implantation, the tensile stress will be simultaneously produced. As a result, the tensile stress due to the expansion of Si substrate contributes to the increase of PMA via the negative magnetostriction of polycrystalline NiZn ferrite. The g_{eff} reveals the same trend. The g_{eff} driven by microscopic magnetic interactions inside the materials including the interparticle magnetic dipole interaction and the superexchange interaction increases dramatically when ion dose is higher than 5×10^{14} ions/cm^2. The dipole interaction among these particles are responsible for the increase of g_{eff}, and the magnitude of this interaction is inversely proportional to the cube of average interparticle distance [33–36]. For the irradiated samples, the expansion of the substrate increases the distance between the columnar grains, which results in the decrease of the magnetic dipole interaction among the columnar grains. So the g_{eff} should be reduced with the increasing irradiation dose. On the other hand, the superexchange interaction between magnetic ions through the oxygen ions can reduce the g_{eff} [33,34]. The magnitude of this interaction is determined by the relative position of the metallic and oxygen ions. When the distances between the metallic ions and oxygen ions are shorter and the included angle between these two metal–oxygen bonds is closer to 180°, the superexchange interaction is stronger. In our experimental data, the increase of the lattice parameter of the ferrite results in the decrease of superexchange interaction and the increase of the g_{eff}. In conclusion, the magnetic dipole interaction among the columnar grains and the superexchange interaction contribute to the variation of g_{eff}.

4. Conclusions

In summary, we have investigated morphology, structure and magnetic properties of 200 nm thick $Ni_{0.45}Zn_{0.55}Fe_2O_4$ thin films treated by proton irradiation. The thickness and surface morphology does not change after irradiation, but an unsmooth interface and a 300 nm rough defect layer are formed in the Si substrate after proton irradiation. The lattice parameter increases slightly with the increasing irradiation dose. H_c increases dramatically when the radiation dose exceeds 5×10^{14} ions/cm^2. The reason for the increase of H_c is the enhancements of the mutual diffusion and the stress. The PMA increases significantly when the radiation dose is higher than 5×10^{14} ions/cm^2. The reason is that the stress in the substrate can be tuned by proton implantation, and this stress does naturally influence the magnetic anisotropy via the negative magnetostriction of polycrystalline NiZn ferrite. Lattice expansion and the decrease of the magnetic dipole interaction between the columnar grains results in the variation of the g_{eff}.

Our work suggests that the H_c, the magnetic anisotropy and the g_{eff} of polycrystalline ferrite thin films can be flexibly tuned by proton irradiation. This finding indicates the influence of interface on the magnetic properties of NiZn ferrite thin films treated by proton irradiation, which can enrich our capacity of manipulating the magnetic properties for potential applications.

Acknowledgments

This work is supported by the National Basic Research Program of China (Grant Nos. 2010CB832904 and 2012CB933101), the National Natural Science Foundation of China (Grant Nos. 51371093, 11034004 and 51202102), Program for Changjiang Scholars and Innovative Research Team in University (Grant No. IRT1251), and Specialized Research Fund for the Doctoral Program of Higher Education (Grant No. 20130211130003).

References

[1] J.P. Singh, G. Dixit, H. Kumar, R.C. Srivastava, H.M. Agrawal, R. Kumar, Formation of latent tracks and their effects on the magnetic properties of nanosized zinc ferrite, J. Magn. Magn. Mater. 352 (2014) 36–44.
[2] E. Kita, K.Z. Suzuki, Y. Liu, Y. Utsumi, J. Morishita, D. Oshima, T. Kato, T. Niizeki, K. Mibu, H. Yanagihara, Magnetization control for bit pattern formation of spinel ferromagnetic oxides by Kr ion implantation, J. Appl. Phys. 115 (2014).
[3] J. Sun, Z. Wang, Y. Wang, Y. Zhu, L. Pang, T. Shen, F. Li, Structural and magnetic properties studies on swift heavy ion (SHI) irradiated Fe_3O_4 thin films, Nucl. Instr. Meth. B 286 (2012) 277–281.
[4] H. Song, D. Park, Structural and magnetic studies on the enhancement of the giant magnetoimpedance by ion irradiation, Thin Solid Films (2011).
[5] D.K. Shukla, R. Kumar, S. Mollah, R.J. Choudhary, P. Thakur, S.K. Sharma, N.B. Brookes, M. Knobel, Swift heavy ion irradiation induced magnetism in magnetically frustrated BiMn_{2}O_{5} thin films, Phys. Rev. B 82 (2010) 174432.
[6] J. McCord, L. Schultz, J. Fassbender, Hybrid soft-magnetic lateral exchange spring films prepared by ion irradiation, Adv. Mater. 20 (2008) 2090–2093.
[7] C. Chappert, H. Bernas, J. Ferre, V. Kottler, J.P. Jamet, Y. Chen, E. Cambril, T. Devolder, F. Rousseaux, V. Mathet, Planar patterned magnetic media obtained by ion irradiation, Science 280 (1998) 1919–1922.
[8] S. Kim, S. Lee, J. Ko, J. Son, M. Kim, S. Kang, J. Hong, Nanoscale patterning of complex magnetic nanostructures by reduction with low-energy protons, Nat. Nano. 7 (2012) 567–571.

[9] T. Tsutaoka, Frequency dispersion of complex permeability in Mn–Zn and Ni–Zn spinel ferrites and their composite materials, J. Appl. Phys. 93 (2003) 2789–2796.
[10] Z. Beji, S. Ammar, L. Smiri, M.-J. Vaulay, F. Herbst, B. Gallas, F. Fievet, Spray deposition of nanocrystalline Ni1− $xZn_xFe_2O_4$ ($x \leqslant 0.6$) films from polyol-mediated sol: Microstructure and magnetic properties, J. Appl. Phys. 103 (2008) 07E744.
[11] T. Nakamura, Snoek's limit in high-frequency permeability of polycrystalline Ni–Zn, Mg–Zn, and Ni–Zn–Cu spinel ferrites, J. Appl. Phys. 88 (2000) 348–353.
[12] A. Verma, T. Goel, R. Mendiratta, R. Gupta, High-resistivity nickel–zinc ferrites by the citrate precursor method, J. Magn. Magn. Mater. 192 (1999) 271–276.
[13] L. Kong, Z. Li, G. Lin, Y. Gan, Ni-Zn ferrites composites with almost equal values of permeability and permittivity for low-frequency antenna design, Magn. IEEE Trans. 43 (2007) 6–10.
[14] J. Sevick, Magnetic materials for broadband transmission line transformers, High Freq. Electron. 4 (2005) 46–51.
[15] M.C. Chhantbar, K.B. Modi, G.J. Baldha, H.H. Joshi, R.V. Upadhyay, R. Kumar, Influence of 50 MeV Li^{3+}-ion irradiation on structural and magnetic properties of Ti^{4+}-substituted $Li_{0.5}Al_{0.1}Fe_{2.4}O_4$, Nucl. Instr. Meth. B 244 (2006) 124–127.
[16] W.L. Jiang, J.A. Sundararajan, T. Varga, M.E. Bowden, Y. Qiang, J.S. McCloy, C.H. Henager, R.O. Montgomery, In situ study of nanostructure and electrical resistance of nanocluster films irradiated with ion beams, Adv. Funct. Mater. 24 (2014) 6210–6218.
[17] D.W. Guo, Z.M. Zhang, M. Lin, X.L. Fan, G.Z. Chai, Y. Xu, D.S. Xue, Ni-Zn ferrite films with high resonance frequency in the gigahertz range deposited by magnetron sputtering at room temperature, J. Phys. D-Appl. Phys. 42 (2009).
[18] J.F. Ziegler, M. Ziegler, J. Biersack, SRIM – the stopping and range of ions in matter (2010), Nucl. Instr. Meth. B 268 (2010) 1818–1823.
[19] A. Verma, T. Goel, R. Mendiratta, P. Kishan, Magnetic properties of nickel–zinc ferrites prepared by the citrate precursor method, J. Magn. Magn. Mater. 208 (2000) 13–19.
[20] M. Sorescu, L. Diamandescu, R. Peelamedu, R. Roy, P. Yadoji, Structural and magnetic properties of NiZn ferrites prepared by microwave sintering, J. Magn. Magn. Mater. 279 (2004) 195–201.
[21] C. Braley, F. Mazen, A. Tauzin, F. Rieutord, C. Deguet, E. Ntsoenzok, Si exfoliation by MeV proton implantation, Nucl. Instr. Meth. B 277 (2012) 93–97.
[22] C. Braley, F. Mazen, A.M. Papon, A.M. Charvet, F. Rieutord, E. Ntsoenzok, Fracture in (100) Si after high energy protons implantation, Phys. Status Solidi C 9 (2012) 2023–2026.
[23] M. Weldon, V. Marsico, Y. Chabal, A. Agarwal, D. Eaglesham, J. Sapjeta, W. Brown, D. Jacobson, Y. Caudano, S. Christman, On the mechanism of the hydrogen-induced exfoliation of silicon, J. Vac. Sci. Technol., B 15 (1997) 1065–1073.
[24] T. Akatsu, K.K. Bourdelle, C. Richtarch, B. Faure, F. Letertre, Study of extended-defect formation in Ge and Si after H ion implantation, Appl. Phys. Lett. 86 (2005).
[25] P.J. Schultz, C. Jagadish, M. Ridgway, R. Elliman, J. Williams, Crystalline-to-amorphous transition for Si-ion irradiation of Si (100), Phys. Rev. B 44 (1991) 9118.
[26] L.A. Marqués, L. Pelaz, M. Aboy, L. Enríquez, J. Barbolla, Microscopic description of the irradiation-induced amorphization in silicon, Phys. Rev. Lett. 91 (2003) 135504.
[27] A. Battaglia, S. Campisano, Mechanisms of amorphization in crystalline silicon, J. Appl. Phys. 74 (1993) 6058–6061.
[28] L. Li, S.X. Wang, K.-P. Hwang, Y. Min, M. Mao, T. Schneider, R. Bubber, Package compatibility and substrate dependence of granular soft magnetic material CoFeHfO developed by reactive sputtering, J. Appl. Phys. 99 (2006). 08M301–308M301-303.
[29] M. Li, G.-C. Wang, H.-G. Min, Effect of surface roughness on magnetic properties of Co films on plasma-etched Si (100) substrates, J. Appl. Phys. 83 (1998) 5313–5320.
[30] J.-K. Lee, Y. Lin, Q.X. Jia, T. Höchbauer, H.S. Jung, L. Shao, A. Misra, M. Nastasi, Role of strain in the blistering of hydrogen-implanted silicon, Appl. Phys. Lett. 89 (2006) 101901.
[31] H. Suhl, Ferromagnetic resonance in nickel ferrite between one and two kilomegacycles, Phys. Rev. 97 (1955) 555.
[32] J. Smith, Beljers, Ferromagnetic resonance of absorption in $BaFe_{12}O_{19}$ a highly anisotropy crystal, Phillips Res. Rep. 10 (1955) 113–115.
[33] T. Komatsu, N. Soga, ESR and Mössbauer studies of the precipitation process of various ferrites from silicate glasses, J. Mater. Sci. 19 (1984) 2353–2360.
[34] T. Komatsu, N. Soga, M. Kunugi, ESR study of $NiFe_2O_4$ precipitation process from silicate glasses, J. Appl. Phys. 50 (1979) 6469–6474.
[35] T. Komatsu, N. Soga, ESR and Mössbauer studies of crystallization process of sodium iron silicate glass, J. Chem. Phys. 72 (1980) 1781–1785.
[36] Y. Sui, D. Xu, F. Zheng, W. Su, Electron spin resonance study of $NiFe_2O_4$ nanosolids compacted under high pressure, J. Appl. Phys. 80 (1996) 719–723.